PERFORMANCE ANALYSIS OF SERVO MOTOR CONTROL IN FULLY ELECTRIC INJECTION MOLDING MACHINES

PHÂN TÍCH HIỆU SUẤT ĐIỀU KHIỂN ĐỘNG CƠ SERVO TRONG MÁY ĐÚC ÉP PHUN HOÀN TOÀN BẰNG ĐIỆN

Thanh Khanh Cao, Doan Hung Vo, Van Thanh Hoang*

The University of Danang - University of Science and Technology, Vietnam

*Corresponding author: hvthanh@dut.udn.vn

(Received: May 08, 2025; Revised: November 20, 2025; Accepted: November 21, 2025)

DOI: 10.31130/ud-jst.2025.23(11).263E

Abstract - Fully electric IMMs are replacing hydraulic presses due to higher energy efficiency, lower emissions, and improved motion precision, where the servo motor is crucial. This study develops a dynamic model of the screw-driven injection unit and a transfer function for closed-loop control in MATLAB/Simulink. A new injection strategy uses optimized PI regulation to minimize position and velocity errors. Experiments under identical loads compare the method with the standard servo drive of a FANUC IMM and a conventional induction motor system. Results show marked reductions in angular deviation, overshoot, and velocity fluctuation. The study also quantifies static friction effects on achievable injection speed, providing design references for high-precision, energy-saving IMM systems.

Key words - Fully electric IMM; Injection unit; Servo motor; Matlab Simulink; Response simulation

Tóm tắt - Máy ép nhựa điện (IMM) đang thay thế máy ép thủy lực nhờ tiết kiệm năng lượng, thân thiện môi trường và điều khiển chính xác cao, với động cơ servo là trung tâm. Nghiên cứu này xây dựng mô hình động lực học của cụm phun trục vít và phát triển hàm truyền phục vụ điều khiển vòng kín trong Matlab/Simulink. Một chiến lược điều khiển phun mới dùng bộ điều chỉnh PI tối ưu được đề xuất để giảm sai số bám vị trí và vận tốc. Thực nghiệm được tiến hành trong cùng điều kiện tải, so sánh phương án đề xuất với hệ servo chuẩn trên máy Fanuc và hệ truyền động dùng động cơ cảm ứng. Kết quả cho thấy sai lệch góc quay, vượt đỉnh và dao động vận tốc phun giảm rõ, vận tốc ổn định và bám tốt hơn. Nghiên cứu cũng định lượng ảnh hưởng của ma sát tĩnh lên tốc độ phun, cung cấp cơ sở tối ưu điều khiển và thiết kế hệ thống phun chính xác, tiết kiệm năng lượng.

Từ khóa - Máy đúc ép phun điện; Cụm phun; Động cơ Servo; Matlab Simulink; Mô phỏng đáp ứng

1. Introduction

Nowadays, there are multifarious plastic products around us, plastic ranges from intricate products such as parts used in motorcycles, cars, and airplanes to simple household products and school supplies with a vast range of designs and colors [1, 2]. Plastic is even used to substitute materials such as steel, aluminum, copper, and wood,... as a result of many advantages such as being light, durable, tough, and can be reused or recycled [3]. This means that plastic has played an essential role in people's lives. To satisfy those needs, there are more and more methods to make plastic products, typically injection molding techniques (IMT) [4]. Along with the advent and robust evolution of plastic materials as well as IMT, the equipment and machinery in this field are becoming more and more contemporary, and the capacity is advancing. Thereby, IMT can create all sorts of products required by the market with involved geometries and high-dimensional accuracy [2].

The product accuracy of the injection molding machine (IMM) depends on three key factors that are the machine's accuracy [5], the molding accuracy [6], and process parameters [7, 8]. This paper just focuses on the injection unit's accuracy. According to the investigation of the injection unit, there are three manners to control the injection unit, which are controlling through hydraulic systems, only using servo motors, or a combination of both. A hydraulic IMM operates based on a hydraulic system, which contains pumps, valves, motors, pipelines, and an oil tank,... These embodiments show that the machine works mainly on the hydraulic system. The hydraulic cylinder provides the movement of opening and closing the mold through the connecting rod system to amplify the clamping force. This machine has a relatively fast mold closing speed and a low cost. However, during operation, the machine makes noise, and the accuracy is not too high.

The fully electric IMM has movements generated by servo motors. In this IMM, there will be two major controlling parts: the control for the clamping unit and the control for the injection unit. In addition, a servo motor can be used to push products out of the mold. In the injection unit, there will be three servo motors: one to drive the screw to rotate for material feeding, one to push the screw forward to inject plastic into the mold, and the last one to move the whole injection unit to let the nozzle head touch the stationary plate. In particular, the servo motor that drives the screw is the foremost element affecting the product precision [9]. This machine is fairly economical in terms of power consumption (50 - 70%) [10], and its weight is usually smaller than hydraulic IMMs of identical size and features. Nevertheless, the expense of a fully electric IMM is higher than a hydraulic IMM. The advantages of this option are that the molding clamping force is enormous, the productivity is heightened, the clamping unit moves speedily, the molding clamping mechanism has good self-locking properties, so it maintains the mold is clamped stably, and the preciseness in the injection process is elevated [11].

Worldly, scientific papers and documents on plastic IMMs are mainly about hydraulic IMMs or a combination of servo motors and hydraulics; on the other hand, the specific research papers on fully electric plastic IMM are still limited. This paper presents several key contributions. A dynamic model of the screw-driven injection unit is established, and the closed-loop transfer function of the servo motor is derived using Matlab/Simulink, providing a detailed mathematical representation seldom reported in previous studies. An optimized PI control strategy is developed to minimize position and velocity tracking errors, thereby enhancing injection accuracy. Experimental validation under identical conditions benchmarks the proposed approach against a standard Fanuc all-electric injection molding machine and conventional induction systems. In addition, a parametric analysis quantifies the influence of static friction on injection speed, addressing an often-overlooked factor in prior research. After all, this paper aims to construct a research paper on the fully electric plastic IMM to serve the research and production of plastic IMMs.

2. Research method

2.1. Problem statement

Prior studies on the quality monitoring and management of the injection molding process focus on four major subjects, namely process parameters, machine management, process management, and quality management [12]. These studies have displayed that the process parameters have a more extreme influence on the molded part quality than the machine management or process management settings, which are intended to have a more instantaneous impact on the repeatability of the molding quality. Thus, adequate methods for determining the proper process parameters for assuring the production of eligible elements in mass-production settings are urgently required. Kurt et al. [13] have indicated the results of their study that cavity pressure and mold temperature are the predominant factors deciding the quality of the final product in plastic injection molding. Fung et al. [14] have found that melt temperature is the predominantly influential parameter in the product properties of both yield stress and elongation. Tsai et al. [15] have shown the result through experimental and theoretical analysis; the main influential process parameters affecting surface waviness are the melt temperature, followed by mold temperature, injection pressure, and packing pressure. Yu et al. [16] likewise depicted the process parameters definition based on the geometric characteristics of the mold compared to conventional methods; the use of the molding features provided a more precise and susceptible prognosis of the pertinent process parameters.

Products of the IMM perhaps appear with common defects on both the outside of the product, such as warping, short shots, flash, scratches, settlements, weld lines, etc. And also inside the product, such as cracks, vacuum pitting, delamination, etc. For each defect, there are several methods to prevent them by adjusting the process parameters, which are injection velocity, injection pressure, material temperature, mold temperature, cooling time, and V/P switchover, etc. To modify almost these process parameters, the machine has to be controlled by a high-precision transmission system.

2.2. Limitations of previous studies

Although injection molding machines (IMMs) have been widely studied, most prior research has focused on hydraulic or hybrid hydraulic–servo systems, while comprehensive investigations of fully electric IMMs remain limited. Key research gaps can be identified.

First, the effects of friction, particularly static friction, have often been overlooked, leading to reduced accuracy in predicting injection velocity, packing pressure, and dimensional stability.

Second, many studies rely mainly on mathematical modeling and numerical simulation without sufficient experimental validation, which limits their practical applicability.

Third, research on servo motor behavior in fully electric IMMs remains inadequate, as most existing works lack quantitative analyses of how the screw-driving servo influences product quality.

Finally, comparative evaluations among hydraulic, hybrid, and fully electric IMMs are still fragmented, with few systematic assessments of accuracy, energy efficiency, dynamic response, and long-term stability.

Overall, these limitations reveal a significant gap in the comprehensive understanding of fully electric IMMs, highlighting the need for integrated theoretical, simulation, and experimental approaches to evaluate their adaptability and performance.

2.3. Experimental method

2.3.1. Input parameters for the injection process

Supposing the material feeding process is finished, then consider the injection process to guarantee the injection volume. Specific data are as follows: Injection volume (Including the residual amount after injection): $V_{total} = 37.7(cm^3)$; Reality injection volume: $V_R = 29\ (cm^3)$ (Referring to the Fanuc IMM 30 tons); Injection time: $t = 1$ (s); The screw stroke: $S = 100$ (mm); Toothed belt transmission ratio: $u = 3$; Ball screw - nut pitch: $P_h = 12$ (mm).

2.3.2. Simulation software

Currently, there are various responsive simulation software for fluid systems, in this research exerts the MATLAB Simulink to simulate the injection process of IMM. MATLAB Simulink is an environment that helps to support system-level design, simulation, automatic code generation, and continuous test and verification of embedded systems, and also provides a graphical editor, customizable block libraries, and solvers for modeling and simulating dynamic systems based on time.

In this injection process simulation, using the command block follows as Gain block: Amplification calculating the input parameters; Scope block: Shows the system characteristics; Integrator block: Used to implement integral calculations; Derivative block: Used to implement derivative calculations; Measurement block: Used to reduce the interference and increase the system precision.

2.3.3. The servo motor control diagram is being constructed

In principle, a servo motor consists of electrical and mechanical components. The input signal is voltage (V), and the output is the shaft rotation angle. The motor model defines the relationship between current and torque, where torque drives shaft rotation and induces an electromotive force. Key parameters include shaft inertia, viscous friction, armature resistance, and inductance. A closed-loop feedback system connects the motor output to the command circuit, allowing rapid feedback of speed and position. The control signal, derived from the motion control program, enables precise execution of the desired motion.

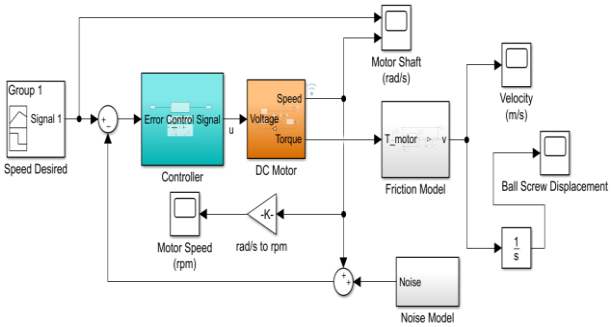

Figure 1. *Schematic diagram of the closed-loop control of a servo motor*

2.3.4. Fabrication of model clusters for the servo motor in the injection unit

To compare the response parameters between servomotors and normal motors, as well as compare process parameters with Fanuc's standard plastic IMMs, the model cluster was built for the purpose of making comparison simulations, it is composed of parts: a servo motor, a normal motor, a ball screw-nut transmission, an encoder, a digital readout, and a PLC programmable controller is shown in Figure 1.

The servo motor has a model: Servo drive ASD-A2-5543-U; Capacity: 2.5 kW; Rotation speed: 1500(rpm). The normal motor has Model: KAYC-IP44; Capacity: 2.5 kW; Rotation speed: 1450(rpm). The ball screw-nut transmission with the screw major diameter $d_1 = 20$ (mm); Ball screw-nut pitch: p = 10 (mm). An encoder with model: E3B2-CWZ6C. A digital readout with stroke: 300(mm); Accuracy ±5μm at 20°C. PLC Programmable controller MITSUBISHI FX1N-60MT-001 for controlling the normal motor, servo motor, and encoder. (1)

During the experiment, the load of the injection unit is evaluated, and the total mass of the injection unit is 50kg, with the ratio of the model being 1/2, as a result, the remaining weight is 25kg.

In addition to the laboratory-scale setup, experimental validation was performed on a fully electric injection molding machine, FANUC S-2000i30A (FANUC Corporation, Japan), used as the benchmark model. The machine features an 18 mm servo-driven injection screw with an injection capacity of ~30 cm³ and a maximum speed of 150 mm/s. Its clamping force is 294 kN (≈30 tons), suitable for manufacturing precision plastic parts.

Benchmark tests were conducted under identical loading and motion conditions to compare the proposed servo-driven model with the FANUC system, focusing on screw displacement, injection velocity, and response time. Both systems operated with the same injection volume (~30 cm³) and stroke (100 mm) to ensure consistency.

Motor position and velocity were recorded via an integrated encoder and monitored using a digital readout system at 1 kHz. Each test was repeated five times, and the mean and standard deviation of injection velocity and position tracking error were computed. The ambient temperature was maintained at 25 ± 1°C to minimize thermal effects.

This setup provides a realistic validation platform for evaluating the proposed servo control strategy under conditions comparable to those of a fully electric injection molding machine.

Figure 2. *Experimental model of the injection unit*

2.3.5. Mathematical method

The relationship between the ball screw-nut rotation angle and the screw stroke is analyzed as follows:

$$H = \frac{P_h}{2\pi}\theta_2 \tag{2}$$

According to (2), it could be rewritten as follows:

$$H = \frac{P_h}{2\pi}\int_0^1 \omega_2 dt \tag{3}$$

Otherwise, the relationship between the ball screw-nut rotation velocity and the rotation angle to the ball screw – nut as follows:

$$\omega_2 = \frac{d\theta_2}{dt}(rad/s) \tag{4}$$

Continue to consider the toothed belt transmission connecting the gear wheel of the motor shaft and the pulley of the ball screw – nut:

$$\omega_1 = u.\omega_2(rpm) \tag{5}$$

The injection speed is calculated by the following formula, which is the derivative of the injection stroke that the screw drives during the time period considered:

$$V_1 = \frac{dH}{dt}(m/s) \tag{6}$$

After calculating and building the formula for the motor rotation velocity, injection stroke, and injection speed, the

following work is testing with the injection flow and injection volume. The formula to calculate the injection flow is:

$$Q = AV_1(m^3/s) \tag{7}$$

According to (5) and (6), they could be rewritten as follows:

$$Q = A\frac{dH}{dt}(m^3/s) \tag{8}$$

The injection volume in 1 second is calculated by the formula as follows:

$$V_R = \int_0^1 Qdt(cm^3) \tag{9}$$

By the formulas (3), (4), (5), (6), (8), and (9), we can build the following injection process model:

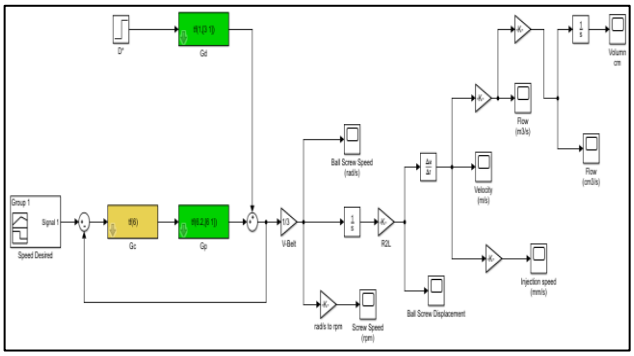

Figure 3. *Injection process calculation model*

From the above mathematical model, build a diagram to determine the injection velocity compared with the Fanuc IMM. The model here considers the interference coefficient K_c, the interference coefficient affecting the pulse to control the number of revolutions of the encoder.

Select the nozzle diameter to be 3mm. We will apply the law of conservation of mass to resolve the injection velocity of the nozzle hole:

$$\rho V_1 S_1 = \rho V_2 S_2 \leftrightarrow V_2 = \frac{V_1 S_1}{S_2}(m/s) \tag{10}$$

According to (6) and (10), the injection velocity of the nozzle varies with time is expressed as follows:

$$V_2 = \frac{S_1}{S_2}\frac{dH}{dt}(m/s) \tag{11}$$

3. Results and discussions

3.1. The consequence of the amplification coefficient on the servo motor

The amplification coefficient is an index that quantifies the likelihood of an increase in power or the signal amplitude from input to output. In turn, changing the value of the amplification coefficient G_C from 1 to 3 over a period of 1 second, the graph is illustrated in Figure 4. From the graph, it can be seen that the larger the amplification coefficient, the faster the response time. Nevertheless, there exists a value of the amplification coefficient, which is the limited amplification coefficient (K_{limit}) if the system amplification coefficient exceeds K_{limit}, it will destabilize the system [17].

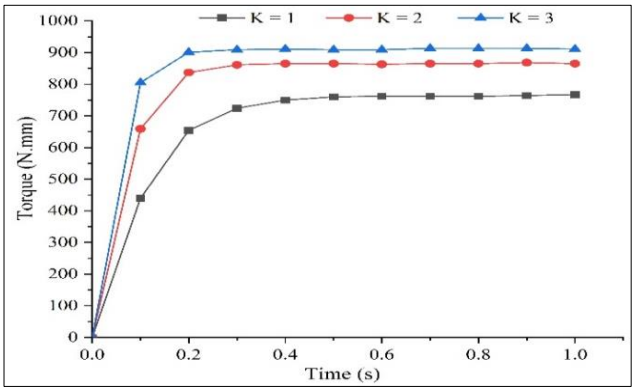

Figure 4. *The consequence of the amplification coefficient on the servo motor torque*

3.2. The effect of the control block on the servo motor torque

The control block is a first-order system. Physically, this system represents an RC circuit. The relationship between the input and output signal is described by the following formula:

$$\frac{C(s)}{R(s)} = \frac{1}{Ts+1} \tag{12}$$

Implementing the Laplace transform of the unit function $\frac{1}{s}$, that is, replacing $R(s) = \frac{1}{s}$ into the formula (11), that formula could be rewritten as follows:

$$C(s) = \frac{1}{Ts+1}.\frac{1}{s} = \frac{1}{s} - \frac{1}{s+\frac{1}{T}} \tag{13}$$

According to the literature [17], the smaller the time constant, the quicker the response of the system. The final result is demonstrated by the following formula:

$$\frac{dc}{dt} = \left|\frac{1}{T}.e^{\frac{-t}{T}}\right|_{t=0} = \frac{1}{T} \tag{14}$$

Changing the control value in the Laplace operator in turn, maintaining the amplification coefficient and the measurement block unchanged, the following response diagram is depicted in Figure 5. Through the graph, it is commented that the more the value of the control variable increases, the slower the response of the servo motor.

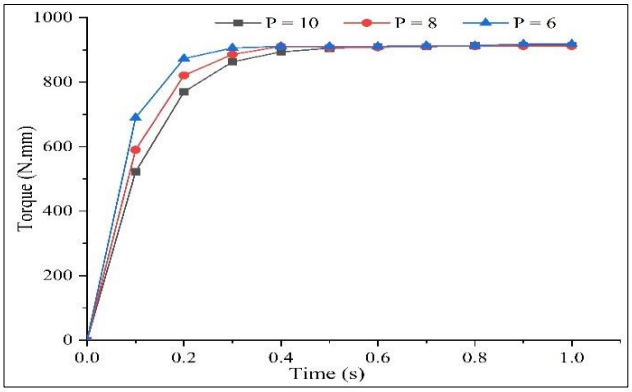

Figure 5. *The effect of the control variable on the servo motor torque*

3.3. The capability to satisfy the parameters of the servo motor

From the formula (2), the rotation angle to the ball screw-nut drive the screw forward 100 mm is calculated as follows:

$$(2) \Leftrightarrow \theta_2 = \frac{2\pi H}{P_h} = \frac{2\pi \times 0.1}{0.012} = 52.4(rad) \quad (15)$$

Based on the formula (4) and solving Eq. (15), with the injection time is 1 second, therefore, the ball screw – nut rotation velocity is computed as below:

$$\omega_2 = 52.4(rad/s) \approx 500(rpm) \quad (16)$$

By the formula (5) and solving Eq. (16), with the toothed belt transmission ratio, the motor rotation velocity is calculated as follows:

$$\omega_1 = 3 \times 500 = 1500(rpm) \quad (17)$$

3.3.1. The responsiveness of the servo motor to the injection process parameters

The specific closed-loop control diagram of the servo motor is shown in Figure 1, at the encoder input signal block, setting the rotation angle for the motor by calculating its rotation angle (rad/s). With the above calculation, the motor speed is 1500 (rpm) ≈ 157 (rad/s). From the above Eqs. (17) and (4), the ball screw-nut rotation velocity with 500 (rpm) and the calculated travel of the screw in 1 1-second period also fulfill the simulated value in the Figure. 6a and Figure. 6b.

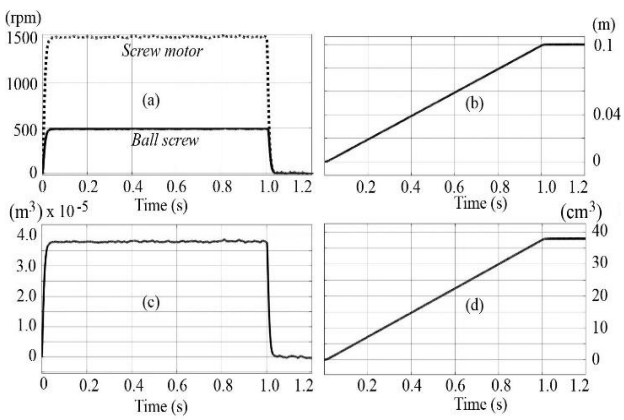

Figure 6. *The rotation velocity of the servo motor and the ball screw-nut (a), the travel stroke of the screw (b), the injection flow of the injection screw (c), and the injection volume (d)*

Similarly, when the values of the servo motor velocity, the ball screw-nut velocity, and screw stroke are met, testing the injection flow and injection volume is executed. Because in the injection process, the screw solely moves in a reciprocating and the diameter of the injection screw on the nozzle side is almost unchanged, accordingly, the identical value of the screw major diameter D_{screw}= 22mm for calculation. To calculate the required injection flow, based on formula (7), it is essential to first calculate the scanning area of the screw and the injection speed, with the injection time is 1 second from formula (8).

$$A = \frac{\pi D_{screw}^2}{4} = \frac{\pi \times 0.022^2}{4} = 0.00038(m^2) \quad (18)$$

$$V_1 = 0.1(m/s) \quad (19)$$

$$\Rightarrow Q = AV_1 = 0.00038 \times 0.1 = 3.8 \times 10^{-5}(m^3/s) \quad (20)$$

From the data (8) and (20), the graph showing the simulated injection flow has the following results: Looking at the graph in Figure 6c, the simulated injection flow value completes the calculation requirements. The injection volume in 1 second is calculated by the formula (9), and from there, the injection volume is satisfied in Figure 6d.

3.3.2. The experiment for the position deviation between the servo motor and the normal motor

Implementing the experimental model on 2 types of motors: Normal motor and servo motor, with each type of motor, will have the same number of revolutions fixed. To determine the number of revolutions of the normal motor, the encoder (1) is used. For servo motors, use a pulse driver to control the number of revolutions.

Fixed the stroke of the screw, corresponding to the displacement of the entire injection unit. In the experimental model, the ball screw-nut type is used (1). Thus, corresponding to one revolution of the lead screw, the nut translates to 10mm. Using a Mitutoyo digital readout (1) to determine the position error, the composition of the digital readout contains a display screen and a position probe to check the position error.

Making a 100mm injection stroke and measuring the position error with the digital readout. After 10 measurements for each type of motor, with the corresponding load, the measurement results are determined as the following figure:

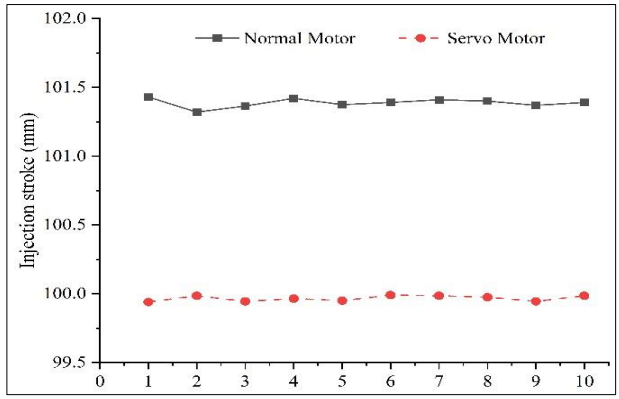

Figure 7. *The position difference between the two kinds of motors*

From Figure 7, collecting data from 10 experiments, calculate the standard deviation of each type of motor. The standard deviations of the servo motor (21) and the normal motor (22) are calculated as follows:

$$s_1 = \sqrt{\frac{\sum_{i=1}^{10}(x_i - \overline{X})^2}{9}} = 0.019 \quad (21)$$

$$s_2 = \sqrt{\frac{\sum_{i=1}^{10}(x_i - \overline{X})^2}{9}} = 0.032 \quad (22)$$

According to solving Eqs. 21 and 22, the position

standard deviation between the two sorts of motors is not more than 5%; therefore, both can be accepted. Nonetheless, the normal motor has a larger position deviation; hence, the volume of plastic supplied to the mold is furthermore proportional to the above position deviation, causing the product to have defects such as vacuum pitting, weld lines, etc.

Weld lines and surface defects are common in plastic molding, often caused by unstable injection speed or inaccurate positioning, especially when using conventional motors. Servo motors offer precise control, ensuring stable filling and cooling, which significantly improves surface quality and part strength.

3.3.3. The experimental determination of injection velocity compared with the Fanuc plastic injection molding machine

The IMM data is taken from Fanuc's catalog, with the IMM model S-2000i30A.

This experimental model only measures the speed of the ball screw-nut (mm/s) driven by the servo motor for a fixed period of 1 second. Corresponding to different time points, the speed of the ball screw-nut will be different. In this study, it is necessary to display the velocity at times from 0.1 – 0.2 – 0.3 – 0.4 – 0.5 – 0.6 – 0.7 – 0.8 – 0.9 – 01 second.

From Eq. (11), which is the equation for calculating the injection velocity at the nozzle hole, a calculation model for the injection velocity has been constructed in Figure 1. The consequences of the injection velocity comparison with the Fanuc injection molding machine are expressed as follows:

Table 1. *Injection velocity when using the servo motor*

Time (s)	Screw velocity (mm/s)	Injection velocity (mm/s)
0.1	0.6	26.67
0.2	3.8	168.91
0.3	7.1	315.60
0.4	11.8	524.51
0.5	15.1	671.20
0.6	16.8	746.76
0.7	18.2	808.99
0.8	18.7	831.22
0.9	18.8	835.66
1.0	18.8	835.66

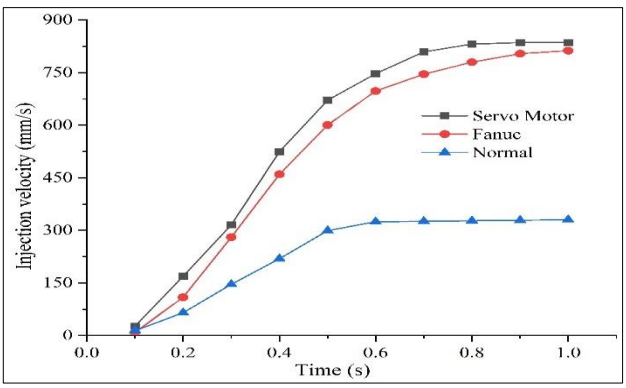

Figure 8. *The injection velocity of the design IMM compared to the Fanuc IMM*

Table 1 and Figure 8 show that with the same period of time, the injection velocity of the servo motor is proximate to the injection velocity of the Fanuc IMM. However, the friction of the injection process and the error of the transmission are not taken into account.

In addition to the above comparison, continuing to compare the injection velocity between experiment and theory, the experimental results are depicted in Figure 9, which indicates the difference in injection velocity between the IMM (Fanuc) and the designed IMM. It can be seen that this difference is due to the fact that in actual production operation, the IMM (Fanuc) has the drag coefficient of the molten material and the friction of the molten plastic. Nevertheless, in this theory and experiment, the drag coefficient of the molten material and other influencing coefficients have not been considered.

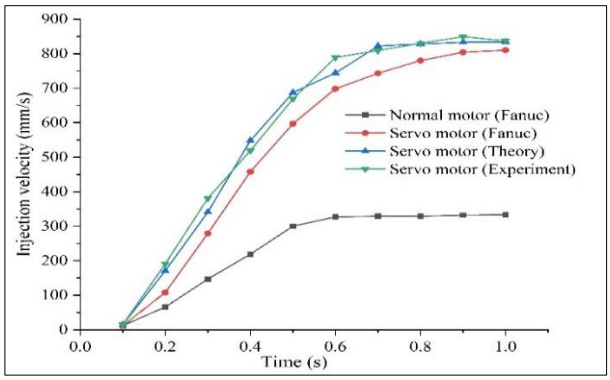

Figure 9. *Injection velocity between experiment and theory*

3.3.4. The effect of the static friction coefficient on injection speed

During the injection phase, molten polymers replicate the mold surface texture to form the desired product [18]. The efficiency of this process depends on various factors, including the properties of the plastic and its molten state. Friction within the molten polymer represents the resistance to its relative motion, while in an injection molding machine, it refers to the resistance between the molten polymer and the contacting metal surfaces.

In the plastic injection process, friction arises from the interaction forces at the contact interfaces. Its magnitude depends on the surface and material properties of the contacting components [9-10]. These forces are difficult to predict, as surface characteristics vary over time due to deformation, wear, separation, or oxidation. The frictional behavior is commonly characterized by the friction coefficient μ, defined as the ratio between the frictional force and the normal load:

$$\mu = \frac{F_f}{N} \tag{23}$$

According to research [17], the friction coefficient of some polymers is presented in Table 2.

Table 2. *The friction coefficient of several polymers*

Polymer	μ_k	μ_s
PP	0.08	0.11
PC	0.34	0.38
ABS	0.30	0.35
PA6	0.22	0.26

In Figure 10, the initial acceleration phase (0.1s to 0.4s), the maximum velocity deviation occurs, where the simulated system shows a significantly greater discrepancy compared to the actual Fanuc machine. This is mainly due to the initial static friction in the Fanuc system not being effectively compensated, resulting in substantial resistive force. When the simulation is performed with a static friction coefficient of $\mu_s = 0.38$, the results closely align with those of the Fanuc system. During the steady-state phase (0.6s to 1s), all velocity curves converge toward the target speed of 800 mm/s, and the velocity deviation gradually decreases. The curve corresponding to a friction coefficient of $\mu_s = 0.38$ provides the closest match to the actual Fanuc machine, both in trend and in absolute values. In terms of settling time, analysis of the graph indicates that the servo system reaches a steady-state velocity in the range of 800 mm/s to 840 mm/s at approximately 0.7 seconds. Prior to this point, the velocity increases rapidly with minimal overshoot. This settling time of 0.7 seconds demonstrates fast dynamic performance, making the system well-suited for high-speed and high-precision applications such as injection molding machines.

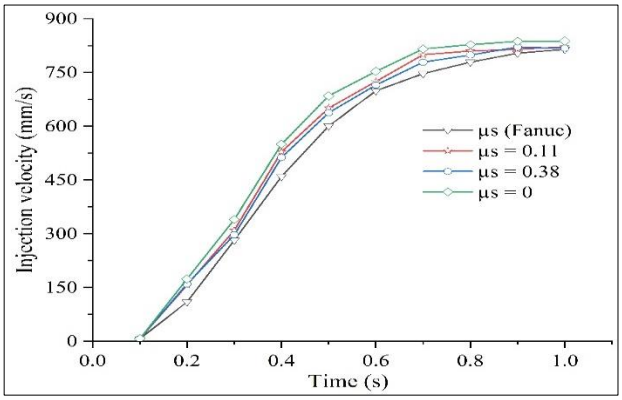

Figure 10. *The effect of static friction coefficient on injection velocity of plastic*

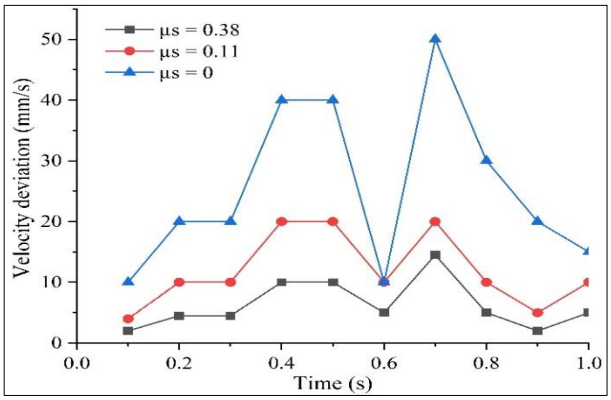

Figure 11. *The injection velocity deviation between the simulation and the Fanuc machine*

The results obtained from the servo motor modeling and experimental validation are directly relevant to the injection molding process. In practice, the servo-driven screw mechanism governs the filling rate, melt pressure, and volumetric consistency of the injected polymer, all of which are critical parameters determining product quality. The improved control accuracy achieved through the optimized PID parameters ensures smoother velocity transitions and more stable pressure profiles during the filling and packing stages. As a result, the melt front advances more uniformly, reducing weld line formation, voids, and air traps. Moreover, the enhanced positional precision of the servo motor minimizes volumetric fluctuations of the injected melt, leading to improved dimensional accuracy and part repeatability. These findings confirm that the proposed control approach is not limited to theoretical modeling but can be directly applied to fully electric injection molding machines to improve surface finish, dimensional stability, and process reliability in actual production environments.

4. Conclusions

The study presented the theoretical and experimental analysis of the injection unit of the plastic IMM based on implementing mathematical and empirical models. When setting the servo motor control model, need to be concerned about the amplification and control coefficients for more reasonable results. It could be seen that there is a difference in the rotation angle of the normal motor and the servo motor when they carry the same load, the same power, and the same number of revolutions. The results show that the normal motor has a larger rotation error than the servo motor. Accordingly, the servo motor is an optimized option over the normal motor for better product quality.

For the experimental model in this study, the injection velocity of the plastic IMM has been calculated indirectly through the travel speed of the ball screw-nut, thanks to the law of conservation of mass. Even though not take into account the influence of the whole friction during injection and the influence of ball screw-nut transmission errors and other factors, the results of the injection velocity of the designed and experimental IMM are approximately equal to those of the Fanuc IMM, and once more shows the outstanding quality of servo motor systems compared with the hydraulic IMM.

Furthermore, the study indicates results on the effect of the static friction coefficient on the injection velocity of IMM. On the other hand, the injection velocity of the IMM also depends on the drag coefficient of the material, and other factors, with different materials having different coefficients [17], with more coefficients analyzed, and more precise results. Future work should integrate more detailed mechanical and material properties to further enhance the performance and accuracy of fully electric plastic injection molding machines.

In addition, this study clearly highlights its novelty by proposing a new control approach with experimentally optimized PI gains, conducting a rare direct benchmarking experiment under identical loading conditions against a Fanuc IMM, and performing a systematic quantitative analysis of the static friction coefficient's effect on injection speed - a factor that has not been explicitly characterized in prior literature. These contributions provide a strong theoretical and experimental basis for future optimization of fully electric IMMs.

Nomenclatures

θ_1: The rotation angle of the motor shaft (deg);

θ_2: The rotation angle to the ball screw - nut drive the screw forward 100 mm (deg);

ω_1: The motor rotation velocity (rpm/min);

ω_2: The ball screw - nut rotation velocity (rpm/min);

V_1: The injection speed (m/s);

V_2: The injection speed of the nozzle hole (m/s);

Q: The injection flow (m^3/s);

A: The scanning area of the screw (m^2);

ρ: Specific weight of the material;

S_1: The area of ball screw – nut (m^2);

S_2: The area of the nozzle hole (m^2);

F_f: The friction force;

N: The surface normal force;

μ_k: The kinetic friction coefficient;

μ_s: The static friction coefficient.

Acknowledgements: The authors sincerely acknowledge Chau Da Co., Ltd. (CDA), No. 2 Street, Hoa Cam Industrial Park, Cam Le Ward, Da Nang City, Vietnam, for its professional support, provision of data, and research facilities, which made a significant contribution to the completion of this paper.

REFERENCES

[1] N. T. P. Pilapitiya and A. S. Ratnayake, "The world of plastic waste: A review", *Cleaner Materials*, vol. 11, p. 100220, 2024. https://doi.org/10.1016/j.clema.2024.100220

[2] H. Fu *et al*., "Overview of injection molding technology for processing polymers and their composites", *ES Materials and Manufacturing*, vol. 8, pp. 3–23, 2020. https://doi.org/10.30919/ESMM5F713

[3] M. Y. Lyu and T. G. Choi, "Research trends in polymer materials for use in lightweight vehicles", *Int. J. Precis. Eng. Manuf.*, vol. 16, no. 1, pp. 213–220, 2015. https://doi.org/10.1007/s12541-015-0029-x

[4] M. Zhao and Z. Tang, "Comprehensive analysis of the injection mold process for complex fiberglass reinforced plastics with conformal cooling channels using multiple optimization method models", *Processes*, vol. 13, p. 2803, 2025. https://doi.org/10.3390/pr13092803

[5] L. V. Duong *et al*., "Computational study on the clamping mechanism in the injection molding machine", *Int. J. Adv. Manuf. Technol.*, vol. 121, pp. 7247–7261, 2022. https://doi.org/10.1007/s00170-022-09817-6

[6] H. V. Thanh *et al.,* "Optimization of cooling channel performance to reduce warpage in the design of tubular injection-molded parts", *The University of Danang – Journal of Science and Technology*, vol. 23, no. 5A, pp. 57–63, 2025. https://doi.org/10.31130/ud-jst.2025.163

[7] H. V. Thanh, L. D. Binh, T. Q. Bang, and C. C. A. Chen, "Mechanical properties of PMMA/PC blend by injection molding process", *Key Engineering Materials*, vol. 863, pp. 67–71, 2020. https://doi.org/10.4028/www.scientific.net/KEM.863.67

[8] V. D. Hung *et al*., "Study on residual stress effects to cracking in the injection molding product: A case study of CPVC male threaded adapter fittings with copper insert", *Trans. Can. Soc. Mech. Eng.*, vol. 49, pp. 421–436, 2025. https://doi.org/10.1139/tcsme-2024-0055

[9] M. Li and Z. Li, "Based on vector control of all-electric injection molding machine control system design", *Adv. Mater. Res.*, vols. 490–495, pp. 2210–2214, 2012. https://doi.org/10.4028/www.scientific.net/AMR.490-495.2210

[10] H. W. Zhang, "Design of open motion control system in fully electrical plastic injection molding machine", *Adv. Mater. Res.*, vols. 291–294, pp. 2767–2770, 2011. https://doi.org/10.4028/www.scientific.net/AMR.291-294.2767

[11] J.-Y. Chen, J.-X. Zhuang, and M.-S. Huang, "Enhancing the quality stability of injection molded parts by adjusting V/P switchover point and holding pressure", *Polymer*, vol. 213, p. 123332, 2021. https://doi.org/10.1016/j.polymer.2020.123332

[12] Z. Chen and L.-S. Turng, "A review of current developments in process and quality control for injection molding", *Adv. Polym. Technol.*, vol. 24, pp. 165–182, 2005. https://doi.org/10.1002/adv.20046

[13] M. Kurt, O. S. Kamber, Y. Kaynak, G. Atakok, and O. Girit, "Experimental investigation of plastic injection molding: Assessment of the effects of cavity pressure and mold temperature on the quality of the final products", *Mater. Des.*, vol. 30, pp. 3217–3224, 2009. https://doi.org/10.1016/j.matdes.2009.01.004

[14] C.-P. Fung, C.-H. Huang, and J.-L. Doong, "The study on the optimization of injection molding process parameters with gray relational analysis", *J. Reinf. Plast. Compos.*, vol. 22, pp. 51–66, 2003. https://doi.org/10.1177/0731684403022001843

[15] K. M. Tsai, C.-Y. Hsieh, and W.-C. Lo, "A study of the effects of process parameters for injection molding on surface quality of optical lenses", *J. Mater. Process. Technol.*, vol. 209, pp. 3469–3477, 2009. https://doi.org/10.1016/j.jmatprotec.2008.08.006

[16] S. Yu *et al*., "Intelligent setting of process parameters for injection molding based on case-based reasoning of molding features", *J. Intell. Manuf.*, vol. 33, pp. 77–89, 2020. https://doi.org/10.1007/s10845-020-01658-y

[17] K. Ogata, *Modern Control Engineering*, 5th ed. Upper Saddle River, NJ, USA: Prentice Hall, 2010.

[18] C. C. Hostert, S. Maas, R. Nordmann, and A. Zürbes, "Dynamic simulation of an injection molding machine", *VDI-Berichte*, vol. 1887, pp. 165–180, 2005.

[19] N. Akasaka, "Synchronous positioning control in pressure control among multi-AC servomotors in injection molding machine", *J. Robot. Mechatron.*, vol. 16, pp. 348–354, 2004. https://doi.org/10.20965/jrm.2004.p0348

[20] C. P. Nwadinobi, I. I. Ezeaku, and V. Ugwu, "Design and fabrication of mini-injection moulding machine for small- to medium-scale plastic processing", *Uniport J. Eng. Sci. Res.*, vol. 4, pp. 25–33, 2019.